7. G. Ya. Gerasimov, "A three-dimensional model of rotational transfers in a diatomic gas," Teplofiz. Vys. Temp., 12, No. 5 (1974).
8. J. A. Lordi and R. E. Mates, "Rotational relaxation in nonpolar diatomic gases," Phys. Fluids, 13, No. 2 (1970).
9. G. Ya. Gerasimov and V. N. Makarov, "On the theory of rotational relaxation in a diatomic gas," Zh. Prikl. Mekh. Tekh. Fiz., No. 1 (1975).
10. N. Taxman, "Classical theory of transport phenomena in dilute polyatomic gases," Phys. Rev., 110, No. 6 (1958).
11. E. A. Mason and L. Monchick, "Heat conductivity of polyatomic and polar gases," J. Chem. Phys., 36, No. 6 (1962).
12. E. E. Nikitin and A. I. Osipov, "Vibrational relaxation in gases," in: Advances in Science and Technology, "Kinetics and Catalysis" Series [in Russian], Vol. 4 (1977).
13. Yu. N. Belyaev, V. A. Polyanskii, I. V. Romashin, and E. G. Shapiro, Mechanics Institute of Moscow State University, Report No. 1802 (1976).
14. G. I. Marchuk, Methods of Computational Mathematics [in Russian], Nauka, Moscow (1977).
15. I. B. Vargaftik, Handbook of the Thermophysical Properties of Gases and Liquids [in Russian], Nauka, Moscow (1972).
16. H. Rabitz and S. H. Lam, "Rotational energy relaxation in molecular hydrogen," J. Chem. Phys., 63, No. 8 (1975).

DYNAMICS OF IMPULSIVE METAL HEATING BY A CURRENT AND ELECTRICAL EXPLOSION OF CONDUCTORS

V. N. Dorovskii, A. M. Iskol'dskii, and E. I. Romenskii

UDC 531;539.5;621.316.5

Most studies of electrical explosion are of an experimental nature and are oriented toward solution of concrete practical problems. In particular, exploding conductors are used as circuit breakers in high power inductive energy storage devices, which are important components of many thermonuclear projects. Electrical explosion is of special interest in attempts to realize variants of so-called inertial thermonuclear synthesis, in which the electrical energy stored in a capacitive storage bank is transferred by a collapsing metal shell without intermediate conversion into light or energetic particles.

Simulation of the processes occurring in impulsive heating of conductors by a current is also of interest in connection with certain experimental behavior which appears anomolous. Namely, it appears that certain phenomenological characteristics of the medium are dependent not only on the thermodynamic variables, but also on the time derivatives of the latter. Thus the specific internal energy [1] and the temperature for commencement of fusion (at constant pressure) [2] become functions of the rate of temperature change; the development of anomalies in conductivity [3] and other properties has been discussed. We are concerned here with experiments having heating times t_h greater than the minimum sound time $t_s = 2r/c_s$ (where r is the conductor radius and c_s is the speed of sound) and the characteristic magnetic diffusion time $t_m = 4\pi\sigma r^2/c^2$ (where σ is the conductivity and c is the speed of light). It is assumed that the first condition ($t_h \gg t_s$) ensures uniformity of the mass density distribution over section, while the second ($t_h \gg t_m$) ensures uniformity of current density, Joulean heat source power, and temperature. However there exist estimates and experimental data which indicate that great care must be used in applying these assumptions in cases where anomalies are present.

Moreover, there is an experimental result available which in the present authors' opinion indicates that the converse is true. This is that flexing instabilities related to axial stresses can develop in a deenergized conductor a long time after the completion of the heating stage. For example, in [4] a copper conductor 1 mm in diameter was heated for 20 μsec, and marked instability appeared only after 100 μsec. These facts suggest

Moscow. Translated from Zhurnal Prikladnoi Mekhaniki i Tekhnicheskoi Fiziki, No. 4, pp. 10-25, July-August, 1983. Original article submitted June 21, 1982.

 0021-8944/83/2404-0454$07.50

TABLE 1

	I_{max}, kA	$2R_0$, cm	t_h, sec	t_m/t_h	t_g/t_h	$j_{max} \times 10^{-7}$, A/cm²	$\dot{\varepsilon} \cdot 10^{-5}$, 1/sec
1	6,2	0,0145	1,25	0,25	0,025	3,6	2
2	49,6	0,058	5	1	0,025	1,8	0,5
3	99,2	0,058	1,25	4	0,1	3,6	2

consideration of the problem of impulsive heating of a conductor by a current within the framework of the mechanics of a viscous thermoelastic continuous medium with stress relaxation.

Calculation results were compared basically with the experimental data of [5], which carefully processed the raw data and tested the statistical significance of a number of observed principles upon which experimenters still disagree. Foremost of these are reduction in the slope of the resistance/energy curve recorded in pulse experiments, and change (in the same coordinates) of the point at which fusion commences.

1. Formulation of the Problem. To describe the behavior of a conductor under the action of electrical current it is necessary to consider the equations of elastoplastic deformation simultaneously with the Maxwell equations. As in magnetic hydrodynamics [6] displacement currents are neglected. The Maxwell relaxation model [7] was chosen to describe the dynamics of elastoplastic deformation, since it permits description of continuous transition of the medium from an elastic to a plastic to a liquid state. The complete system of equations in Cartesian coordinates x_i consists of the laws of conservation of energy and momentum, the equations of deformation evolution, and the equations of magnetic field diffusion:

$$n\frac{du_i}{dt} = \frac{\partial \sigma_{ik}}{\partial x_k} + \frac{1}{c}[\mathbf{j}\times\mathbf{H}]_i, \quad \mathbf{j} = \frac{c}{4\pi}\operatorname{rot}\mathbf{H},$$

$$\frac{dg_{ik}}{dt} + g_{i\alpha}\frac{\partial u_\alpha}{\partial x_k} + g_{k\alpha}\frac{\partial u_\alpha}{\partial x_i} = \varphi_{ik},$$

$$\frac{\partial \mathbf{H}}{\partial t} = \operatorname{rot}[\mathbf{u}\times\mathbf{H}] - \frac{c^2}{4\pi}\operatorname{rot}\left(\frac{1}{\sigma}\operatorname{rot}\mathbf{H}\right), \quad \operatorname{div}\mathbf{H} = 0,$$

$$\frac{\partial}{\partial t}\left(n\left(e + \frac{|\mathbf{u}|^2}{2}\right) + \frac{|\mathbf{H}|^2}{8\pi}\right) + \operatorname{div}\mathbf{q} = 0,$$

$$q_i = nu_i\left(e + \frac{|\mathbf{u}|^2}{2}\right) - u_\alpha\sigma_{i\alpha} + \frac{c^2}{4\pi}[\mathbf{E}\times\mathbf{H}]_i - \varkappa\frac{\partial T}{\partial x_i}, \quad \mathbf{E} = \frac{1}{\sigma}\mathbf{j} - \frac{1}{c}[\mathbf{u}\times\mathbf{H}]. \tag{1.1}$$

Here $d/dt = \partial/\partial t + u_\alpha\partial/\partial x_\alpha$; $\mathbf{u} = (u_1, u_2, u_3)$ is the velocity vector; $\sigma_{ik} = 2ng_{i\alpha}\partial e/\partial g_{\alpha k}$ is the stress tensor; g_{ik} is the tensor of effective elastic deformation; $e = e(g_1, g_2, g_3, S)$ is the internal energy density; g_i are the main values of the tensor g_{ik}.

S is the entropy; $n = n_0(\det\|g_{ik}\|)^{1/2}$ is the density of the medium; $T = \partial e/\partial S$ is the temperature; $\mathbf{H} = (H_1, H_2, H_3)$ is the magnetic field vector; σ is conductivity; φ_{ik} are Maxwell relaxation terms; $\varkappa$ is the thermal conductivity coefficient; and c is the speed of light.

We will consider a cylindrical conductor passing an ac current specified by $I(t) = I_{max}\cdot\sin\omega t$. This corresponds to the situation where the wave impedance of the circuit is significantly higher than both its ohmic resistance and the conductor resistance. Consideration of the more general case in which the conductor parameters affect the behavior of the source introduces needless complications. The z axis of a cylindrical coordinate system r, φ, z coincides with the axis of symmetry of the conductor. For the case of axial symmetry, and without consideration of z-dependence, in such a coordinate system Eq. (1.1) appears as

$$r\frac{\partial n}{\partial t} + \frac{\partial rnu}{\partial r} = 0,$$

$$r\frac{\partial nh_2}{\partial t} + \frac{\partial rnuh_2}{\partial r} = nu - \frac{rn}{\tau}\left(h_2 - \frac{h_1+h_2+h_3}{3}\right),$$

$$r\frac{\partial nh_3}{\partial t} + \frac{\partial rnuh_3}{\partial r} = -\frac{rn}{\tau}\left(h_3 - \frac{h_1+h_2+h_3}{3}\right),$$

$$r\frac{\partial nu}{\partial t} + \frac{\partial r\left(nu^2 - \sigma_r + H^2/(8\pi)\right)}{\partial r} = -\left(\sigma_\varphi + \frac{H^2}{4\pi}\right),$$

$$\frac{\partial H}{\partial t}+\frac{\partial}{\partial r}\left(uH-\frac{c^2}{4\pi\sigma r}\frac{\partial rH}{\partial r}\right)=0,$$

$$r\frac{\partial}{\partial t}\left(n\left(e+\frac{u^2}{2}\right)+\frac{H^2}{8\pi}\right)+\frac{\partial}{\partial r}r\left(nu\left(e+\frac{u^2}{2}\right)-u\sigma_r+\frac{uH^2}{4\pi}-\frac{c^2}{16\pi^2}\frac{H}{\sigma r}\frac{\partial rH}{\partial r}-\varkappa\frac{\partial T}{\partial r}\right)=0, \tag{1.2}$$

where u is the radial velocity; $\sigma_r = n\partial e/\partial h_1$, $\sigma_\varphi = n\partial e/\partial h_2$, $\sigma_z = n\partial e/\partial h_3$ are the stresses along the r, φ, z axes (tangent stresses are absent); h_1, h_2, h_3 are the main values of the Henk elastic deformation tensor ($h_i = -(1/2)\ln g_i$) along the axes r, φ, z; H is the azimuthal magnetic field component; $n = n_0 \exp(-h_1 - h_2 - h_3)$ is the density; $\tau(h_1, h_2, h_3, S)$ is the tangent stress relaxation time, which may vary from ∞ (corresponding to a nonlinear-elastic medium) to 0 (an ideal liquid).

The boundary conditions for the problem are as follows:

$$H|_{r=R(t)} = 2I(t)/cR(t),\ H|_{r=0} = 0,$$
$$\sigma_r|_{r=R(t)} = 0,\ \partial T/\partial r|_{r=0} = \partial T/\partial r|_{r=R(t)} = 0$$

(R(t) is the variable radius of the outer conductor boundary).

To complete the system of equations it is necessary to specify an equation of state $e(h_1, h_2, h_3, S)$, relaxation time $\tau(h_1, h_2, h_3, S)$, electrical conductivity coefficient $\sigma(n, S)$, and thermal conductivity coefficient $\varkappa$. The equation of state used was of the form (obtained by interpolation of expressions from [8])

$$e=\frac{K_0}{2\alpha_0^2}\left[\left(\frac{n}{n_0}\right)^{\alpha_0}-1\right]^2+c_t^2\left(\frac{n}{n_0}\right)^{\beta_0}\sum_{i=1}^{3}\left(h_i-\frac{h_1+h_2+h_3}{3}\right)^2+c_V^0T_0\left(\frac{n}{n_0}\right)^{\gamma_0}\left(\exp\left(S/c_V^0\right)-1\right),$$

where $K_0 = c_l^2 - \frac{4}{3}c_t^2$; c_l, c_t are the longitudinal and transverse speeds of sound; α_0, β_0, γ_0 are constants of the material; c_V^0 is the specific heat.

For the copper conductors considered below the following constant values were chosen:

$$c_l = 4.651\,\text{km/sec}, c_t = 2{,}14\ \text{km/sec},$$
$$c_V^0 = 0.412\ \text{J/g}\cdot\text{deg} \qquad n_0 = 8.9\ \text{g/cm}^3$$
$$T_0 = 300\,\text{K},\ \alpha_0 = 0{,}95,\ \beta_0 = 3{,}14,\ \gamma_0 = 1.91.$$

Conductivity was specified by the expression

$$\sigma = \sigma_0(T_0/T)^x(n/n_0)^y,$$

where $\sigma_0^{-1} = 1.7\cdot10^{-6}\ \Omega\cdot\text{cm}$; x = 1; y = 4.

In certain calculations the relaxation time τ was expressed by [9]

$$\tau=\tau_0\left(\frac{n_0c_t^2}{D_\sigma K_0}\right)^{K(T)-1}\exp\left(\mu\frac{U(T)}{RT}\right),$$

where

$$K(T)=\frac{1}{K_1}\left[\left(\frac{T}{\Theta_0K_2}-1\right)^2+K_3\right]^{-1};$$
$$U(T)=c_l^2\frac{T}{\Theta_0K_4}\left(1-\frac{T}{\Theta_0K_5}\right)K(T),$$

For copper the following values were used: $\mu = 63.54$ g, atomic weight; $R = 8.31\cdot10^7$ g·cm²/(sec²·deg), universal gas constant; $\Theta_0 = 315$°K, Debye temperature; $\tau_0 = 23.98\cdot10^{-5}$ sec, $K_0 = 1.96\cdot10^4$, $K_1 = 0.0184$, $K_2 = 0.955$, $K_3 = 1.902$, $K_4 = 1.4\cdot10^2$, $K_5 = 7.22$, $D_\sigma = (1/\sqrt{2})[(\sigma_r - \sigma_\varphi)^2 + (\sigma_\varphi - \sigma_z)^2 + (\sigma_z - \sigma_r)^2]^{1/2}$, tangent stress intensity. This interpolation expression for τ was selected in [9] to describe experimental dependence of yield point on deformation rate.

A numerical solution of Eq. (1.2) was obtained using Godunov's difference method [10]. We will briefly describe the algorithm without presenting the concrete computation expressions.

System (1.2) is written in divergent form

$$\partial A/\partial t + \partial B/\partial r + F = 0, \tag{1.3}$$

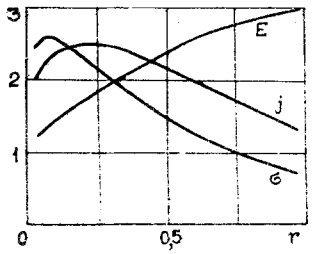

Fig. 1

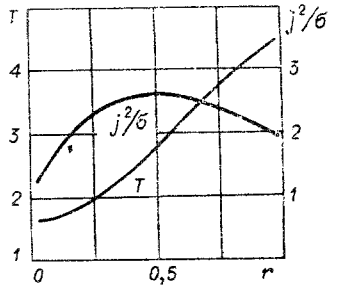

Fig. 2

where

$$A=\begin{Vmatrix} rn \\ rnh_2 \\ rnh_3 \\ rnu \\ H \\ rn\left(e+\frac{u^2}{2}\right)+\frac{H^2}{8\pi} \end{Vmatrix},\quad B=\begin{Vmatrix} rnu \\ rnuh_2 \\ rnuh_3 \\ r\left(nu^2-\sigma_r+H^2/(8\pi)\right) \\ uH-L \\ rnu\left(e+\frac{u^2}{2}\right)-u\sigma_r+\frac{uH^2}{4\pi}-M \end{Vmatrix},$$

$$F=\begin{Vmatrix} 0 \\ -nu+rn\left(h_2-\frac{h_1+h_2+h_3}{3}\right)\Big/\tau \\ rn\left(h_3-\frac{h_1+h_2+h_3}{3}\right)\Big/\tau \\ \sigma_\varphi+H^2/(4\pi) \\ 0 \\ 0 \end{Vmatrix},$$

where $L=\frac{c^2}{4\pi\sigma r}\frac{\partial rH}{\partial r}$; $M=\frac{c^2}{16\pi^2}\frac{H}{\sigma r}\frac{\partial rH}{\partial r}+\varkappa\frac{\partial T}{\partial r}$. If a solution is known at a given moment in time, then for the following step in time a solution can be determined from the integral conservation laws

$$\oint_\Gamma (Adr-Bdt)-\int_\Omega\int Fdrdt=0, \tag{1.4}$$

where Ω is the integration region (computation cell); Γ is the boundary of this region. To determine the solution from the conservation laws it is necessary to know the values of n, h_2, h_3, u, H, S, L, M on the side boundaries of the computation cell. They are determined using the concept of "splitting over physical processes." The original system (1.3) is divided into two independent systems of equations. One of these (a hyperbolic system) describes magnetosonic oscillations in the vicinity of each node of the difference grid. The second (parabolic) system describes processes of magnetic field and temperature diffusion. The interaction of these processes is considered by the conservation laws (1.4).

The hyperbolic system is obtained from Eq. (1.3) by assuming L = 0, M = 0. This system is linearized in the vicinity of each difference grid node, and then by using the solution of the discontinuity decay problem in the acoustical approximation its solution is determined on the lateral boundaries of the computation cell.

The parabolic system appears as follows:

$$\begin{aligned} \frac{\partial H}{\partial t}+w\frac{\partial H}{\partial r}&=\frac{c^2}{4\pi}\frac{\partial}{\partial r}\left(\frac{1}{\sigma r}\frac{\partial rH}{\partial r}\right),\\ \frac{\partial T}{\partial t}+w\frac{\partial T}{\partial r}&=\frac{1}{nc_V(n)\,r}\frac{\partial}{\partial r}\left(r\varkappa\frac{\partial T}{\partial r}\right), \end{aligned} \tag{1.5}$$

where w is the speed of motion of the difference grid nodes. An implicit difference technique was used to solve Eq. (1.5). Using values of H and T obtained by solving Eq. (1.5), the fluxes L and M on the lateral boundaries of the computation cell were determined.

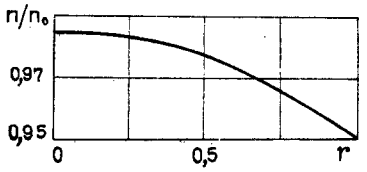

Fig. 3

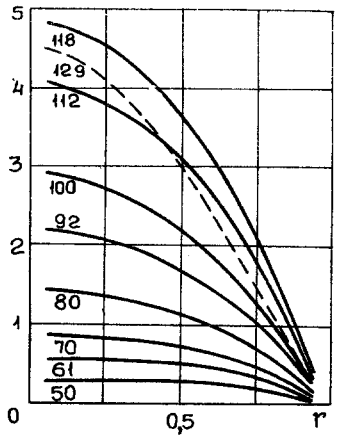

Fig. 4

Knowledge of L and M together with the values obtained from the acoustic discontinuity decay problem permits transition to the next time layer using the integral conservation laws. The calculations described below were performed without consideration of heat transfer processes ($\varkappa = 0$), since they may be neglected in the regimes studied.

In actual experiment the specimen and electrical circuit parameters were chosen such that fusion commenced near the peak of the first half cycle. Simple calculations, confirmed by experiment, show that if the conductor material is not changed, for a constant

$$I_{max}^2 \pi / 2\omega R_0^4 = C_0 \qquad (1.6)$$

a certain form of similarity occurs: Fusion begins with one and the same current phase $I = I_{max} \sin \omega t$. For copper at $C_0 \cong 1.8 \cdot 10^{10}$ $A^2 \cdot sec/cm^4$ the fusion temperature is reached near the first current peak.

Three groups of calculations were performed in which the similarity of Eq. (1.6) was present, and the values of I_{max} (in kA), wire diameter (mm), and heating time $t_h = \pi/2\omega$ (μsec) are shown in Table 1. For all cases shown in the table, the heating time is two orders of magnitude smaller than the thermal diffusion time $t = R_0^2/\chi$ (where R_0 is the conductor radius and χ is the thermal diffusivity) and significantly greater than the sonic time $t_s = 2R_0/c_s$ (where c_s is the speed of sound), 40 times larger in the first and second cases, and 10 times larger in the third. The major difference between the two variants is that in the first the magnetic diffusion time $t_m = 4\pi\sigma R_0^2/c^2$ (where σ is the conductivity and c is the speed of light) is several times smaller than the heating time and skin effects should be slight; in the second case they become significant, and in the third, dominant.

Calculations were performed for each variant in the table using different relaxation times. Moreover, for case 2 relaxation processes were considered in a conductor which was heated rapidly and disconnected. A situation was created similar to that of [11], in which a second thinner wire was installed in series with the main specimen so that current could be interrupted at specified points in time.

2. Ideal Compressible Liquid, Skin Effect, Viscoelasticity. Analysis of the numerical simulation results revealed that some of the principles observed in experiment and regarded as anomalies are naturally explicable within the framework of the local equilibrium model. This dissipation-free model is obtained from Eq. (1.1) if we set the thermal conductivity $\varkappa$ and relaxation time τ equal to zero. We then deal with an ideal compressible liquid.

The distributions of current density, conductivity, and electric field over radius are shown for the strong skin effect regime (case 3 of Table 1) in Fig. 1.

With less clearly expressed skin effects only the amounts by which the quantities fall off radially decrease. The curves of Fig. 1 correspond to times close to the current maximum, when $T(r = 1) = 4.52\ T_0$. At such times the temperature and Joulean heat source specific power profiles have the form shown in Fig. 2. Of interest is the monotonic form of the electric field E(r), which also occurs at preceeding moments in time and in other heating regimes. Also remarkable is the shift in the maximum of the heat source power into the depths of the conductor. The electric field maximum is located on the surface.

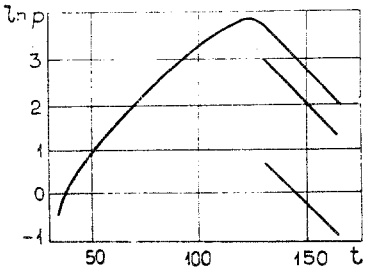

Fig. 5

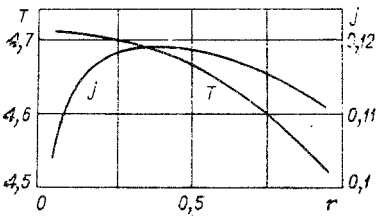

Fig. 6

The dependence of conductivity on density and temperature can be specified in the form

$$\sigma(T,\ n) = \sigma_0(T_0/T)^x(n/n_0)^y,$$

where σ_0, T_0, n_0 are the conductivity, temperature, and density at the initial moment. The results presented correspond to x =1, y =4. For copper, this means that at the point (T_f, n_f) near the fusion temperature σ_0/σ =6.1. Three fourths of the increase in resistivity is then temperature-related, while the remainder is due to the decrease in density produced by expansion.

While in the case of strong temperature skin effect (see Figs. 1, 2) the conductivity and current density profiles are determined basically by T(r), with slower heating, when the temperature is practically constant over radius, the functions σ(r) and j(r) are determined by the density profile n(r), shown in Fig. 3. The change in density from center to surface at the moment when the surface temperature T =4.52 T_0 is (for case 2 of the table) $\delta n/n \cong 3\%$. The temperature change at this time (Fig. 2, curve 1) is $\delta T/T \cong 1.7\%$. The radial behavior of conductivity is essentially determined by the behavior of n(r). The decrease in current density on the surface

$$\delta j/\langle j\rangle = [j(r=1) - \langle j\rangle]/\langle j\rangle \cong -10\%,$$

where <j> is the mean current density over section.

The form of the density (Fig. 3) and pressure (Fig. 4) profiles is a consequence of compressibility and temperature stresses. The high value of these stresses is quite unexpected. Figure 4 illustrates the dynamics of the pressure profile under conditions (case 2) quite close to experiment.

After transient processes are completed, a pressure profile close to parabolic is created. This happenes in approximately 4 μsec (1 μsec before the current peak) when the temperature is still not too high, ∿750°K (T_f =1356°K). In the following stage the process is close to self-similar: The temperature and pressure at the center increase almost exponentially, and the pressure profile remains parabolic. The pressure in the center reaches 5 GPa.

This value is an order of magnitude greater than the "magnetic" pressure $p_m = H^2/(8\pi)$, produced by ponderomotive forces.

We stress that here the characteristic pressure increase time ($\sim 1.4 \times 10^{-6}$ sec) is an order of magnitude greater than the sonic time ($1.5 \cdot 10^{-7}$ sec).

Generation of high temperature stresses is significant in at least two respects: They must be considered in stability problems, and also in phase conversion problems.

The slightly varying pressure profile of Fig. 4 during the heating stage is formed by interaction of temperature effects responsible for a pressure increase, and relaxation processes which lead to unloading. These latter appear clearly when current is terminated abruptly. In Fig. 5 the pressure drop upon termination of current is exponential with a time constant of $0.9 \cdot 10^{-6}$ sec, which is ∿6 times greater than the sonic time. The value of this constant is practically independent of the position of the point on the radius: The upper curve refers to the central zone (r =1/20), the lower to the periphery (r =19/20), and the middle curve to the region near the center (r =13/20). In the relaxation stage $p(r, t) \sim p(r)f(t)$ as compared to the heating stage and the pressure profile readjusts itself so that in a quite large region near the boundary (Δr =0.5-1) the pressure gradient remains practically constant. This readjustment occurs rapidly over a current decay time $\Delta t = 0.5 \cdot 10^{-6}$ sec.

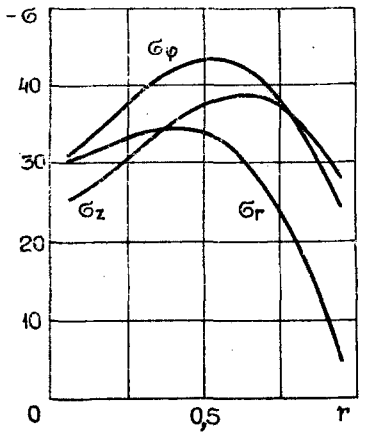

Fig. 7

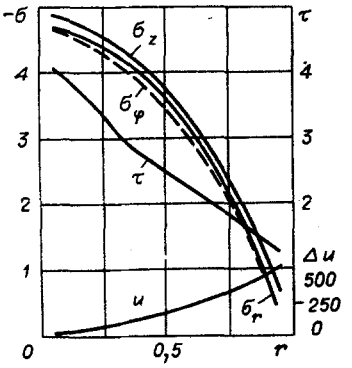

Fig. 8

The form of the pressure profile recorded at times immediately preceeding the beginning of fusion depends significantly on the ratio between heating and magnetic diffusion times. A profile with a maximum at the boundary occurs when skin effects caused by current change with time are significant. Two situations may be distinguished here: a) strong skin effect — the current density and temperature are distributed in a "normal" manner (with minimum at the center); b) moderate skin effect — the temperature has a maximum at the boundary and the current density, at some distance from the boundary. The first case is realized when fusion begins in the first quarter period, long before the current maximum, and in a certain sense is of little interest. The second case was considered in detail above.

When $t_h \gg t_m$ skin effects produced by the time derivative have little effect near the current maximum. In such a regime the distributions of Joulean heat source power density and current density are determined mainly by the mass density profile, which has a minimum near the boundary. Near the time that fusion begins, neither the current density nor temperature have maxima on the boundary. The boundary temperature may even be less than the mean over the section. Figure 6 shows density and temperature profiles at the time when the temperature on the boundary is equal to the fusion temperature at atmospheric pressure. The heating regime corresponds to case 1 of the table.

We note that in all cases (even in the first ($t_h \gg t_m$)) the quantities under consideration have significant radial gradients. This raises a number of questions concerning measurements. In particular we must consider what quantity a sensor signal in fact represents.

The compressible liquid model considered above is unsatisfactory from at least two standpoints: The short time period ($\sim 10^{-6}$ sec) for which stresses exist after completion of the current pulses cannot explain the "delay" of $\sim 10^{-4}$ sec in development of flexion instability [4]; moreover, this time is significantly less than the characteristic thermal conductivity time of [11] ($\sim 10^{-3}$ sec), so that if we give full credit to the model, then in this case after $\sim 10^{-5}$ sec there is a significant superheating of the central portion of the conductor, which despite its significant "lifetime," produces no consequences observable in experiment. Thus it is natural to expand the model by introducing viscosity in some manner.

It is well known that within the framework of nonequilibrium thermodynamics, magnetohydrodynamic flow is described by seven independent phenomenological coefficients, of which five have the sense of tangent viscosity, one has the meaning of volume viscosity, and the final one describes cross interaction [12]. In the present case the situation is simplified by the fact that the flow function reduces essentially to Joulean heating, i.e., in the first approximation it is a source of heat and temperature stresses and the terms of the corresponding equations specific to magnetohydrodynamics are relatively small. Thus one can hope to avoid consideration of the two viscosity effects usually characterized by values of the tangent and volume viscosity.

We must now turn to some model which considers viscosity. The most widely used is the Navier—Stokes model. However we will employ the Maxwell model of a viscoelastic medium [7], considering only effects related to shear stress relaxation.

We will consider volume deformations to be purely elastic. This may be justified to some extent by citing tradition, although we possess no experimental data favoring such an assumption.

The choice of the Maxwell model of a viscous elastic body to relate stresses and deformations is justifiable. Aside from the considerations normally put forward in favor of this model in studies of high speed deformation, we may also note that the model develops in a natural manner from the nonequilibrium statistical thermodynamics of continuous media with a memory and corresponds to the simplest case, exponential decay of the time correlation function for the dissipative momentum flux [13].

Aside from the experimental data collected by the present authors in studying electrical explosion, we can offer the results of [14-16], which also experimentally confirm the validity of this model.

In [14, 15] impulsive heating of a copper surface by an electron beam was studied. Elastoplastic flow corresponding to appearance of well developed slip bands on the irradiated surface was recorded. It was also found that high density dislocation fields form, with development of wedge-shaped deformation twins and twinning dislocations, which is characteristic of shock deformation of a metal. The results were interpreted using a rheological model with hardening, and it was concluded that plastic flow develops upon completion of the heating process.

In [16] deformation ($d\varepsilon/dt = 10^3$-10^4 1/sec) of thin walled aluminum cylinders in a strong magnetic field was studied. The experimental results were compared to calculations using models which described ideally elastoplastic and nonlinear-elastic media and a Maxwell medium with relaxation time from [17]. It was shown that only the last model produced satisfactory agreement with experiment.*

In the calculations presented below an interpolation formula is used for the Maxwell time [9], obtained from analysis of experiments performed under other conditions, both with high speed shock deformation, and with more significant deformations at lower temperatures. Therefore the results must be regarded as approximate.

In order to determine what type of qualitative changes develop as a result of considering Maxwell viscosity, it is natural to consider the case where the relaxation time is significantly greater than the heating time ($\tau \gg t_h$). In a certain sense this limit is an alternate case to that considered above. Calculations with $\tau^{-1} = 0$ were performed for case 3 of the table, for which conventional skin effect produces a temperature profile with significant radial drop (see Fig. 2).

Analysis of the calculation results shows that the transition from $\tau = 0$ to $\tau^{-1} = 0$, as would be expected, affects mainly the character of the stress distribution (Fig. 7). The shapes of the temperature, current density, and conductivity profiles are practically unchanged from Figs. 1, 2. The density at the surface increases somewhat with a slight decrease in expansion rate. As for the stress distribution, $\sigma_r \neq \sigma_\varphi \neq \sigma_z$, with the maximum difference between the components being reached at the surface. We recall that at the surface we require that $\sigma_r = 0$ because of the absence of external surface forces and the neglect of volume viscosity effects.

The absolute value of the longitudinal stress at the surface ($\sigma_z(r = 1) = 2.5$ GPa) is in good agreement with the elementary a priori estimate $\sigma_z \cong \alpha \Delta T E$, where E is Young's modulus. This stress develops mainly because of the absence of deformation (thermal expansion along the z axis).

Figure 8 shows results of stress profile calculations with τ taken from [9] in the prefusion temperature range for case 1 of the table, i.e., when the heating time is significantly greater than the magnetic diffusion time. Also shown are radial distributions of the velocity and tangent relaxation time. The basic principles noted above remain in force here. For example, near the surface ($r = 19/20$) the longitudinal stress value increased from $\sigma_z = 0.17$ GPa for the ideal liquid model to $\sigma_z = 0.68$ GPa for the Maxwell model. In the limit as $t_h \to 0$, if we do not consider effects connected with the density gradient, this quantity can increase to ~ 2 GPa. Decrease in the parameter τ with increase in radius is caused mainly by the increase in tangent stress intensity in this direction, characterized by the stress

*The authors are indebted to G. A. Shneerson for calling their attention to [16].

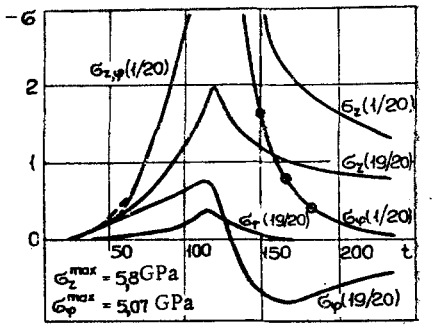

Fig. 9

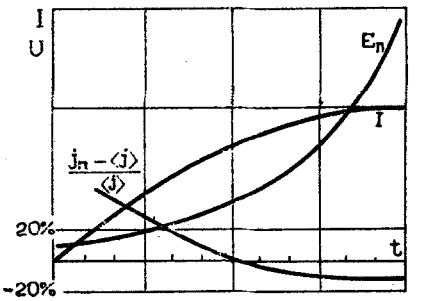

Fig. 10

tensor deviator, since the temperature, upon which τ depends significantly, is practically constant along the radius in this case. The absolute value of the relaxation time varies from $0.4 \cdot 10^{-6}$ sec near the axis to 10^{-7} sec at the boundary.

It was noted above that the stressed state of a conductor heated to prefusion temperatures is maintained for a lengthy ($\sim 10^{-4}$ sec) interval [4]. Generally speaking, this effect may be controlled by either shear or volume relaxation, or both acting together. However the latter has not been considered. Therefore calculations were performed for case 2 of the table (Figs. 3, 4) with a fixed tangent relaxation time $\tau = 10^{-5}$ sec, which for this case is twice the heating time. Just as in Fig. 5, after reaching a maximum in $5.2 \cdot 10^{-6}$ sec, the current was switched off over an interval $\Delta t \cong 0.5 \cdot 10^{-6}$ sec. The calculations encompass the heating period and a time interval of $\sim 10^{-5}$ sec after current switchoff.

For the heating stage the change in the behavior of stress as compared to the ideal liquid model corresponds to that described above. Together with a general increase in stress and temperature there is an increase in σ_z and σ_φ components near the surface. For example, the longitudinal stress at the surface reaches values close to limiting. With respect to the ideal liquid model the remaining parameters change insignificantly.

Of greatest interest is the behavior of stress at the completion of the heating stage. Figure 9 shows stress as a function of time for two points: near the center (r =1/20) and near the surface (r =19/20). In contrast to Fig. 5, the longitudinal stress component in this case relaxes much more slowly, while for the σ_z and σ_φ components the decay constant is practically unchanged ($\sim 0.9 \cdot 10^{-6}$ sec).

Longitudinal stress relaxation is quite different. While in the first case (Fig. 5) the hydrostatic pressure value fell almost exponentially at all points on the radius, in the second case the fall is more gradual, with the characteristic decay time increasing with removal from the center. Thus, for the point r =1/20 the quantity $\left\langle \frac{1}{\sigma} \frac{d\sigma}{dt} \right\rangle^{-1}$ is half of the corresponding value at r =19/20.

Due to "extinction" of σ_r and σ_φ components and equalization of σ_z over radius because of the differences between characteristic decay times, even when only 7 μsec have passed the conductor proves to be compressed along the z axis practically uniformly. At this moment the amplitude of the longitudinal stress is ~0.5 GPa. The complete relaxation time, estimated from the calculated interval, is approximately 30 μsec.

The evolution of σ_φ is of interest. At the beginning of the relaxation stage, as in the previous cases, the sign of σ_φ is negative on the surface and the surface is compressed along this coordinate. Then the value of σ_φ falls to zero, changes sign, and after only ~2 μsec a tensile force of the order of 1 GPa is present.

At the beginning of the relaxation stage the velocity of the boundary maintains its sign and the conductor continues to expand, after which the boundary velocity falls and changes sign.

3. Electrical Measurements and Some Anomalies in Electrical Explosion. We will now consider electrical measurements in greater detail and attempt to explain a number of anomalies in electrical explosion, related in some way or another to electrical measurements.

The main volume of quantitative data on electrical explosion was obtained by performing electrical measurements. Usually two quantities are measured: the total current through

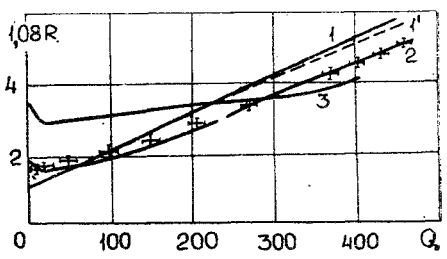

Fig. 11

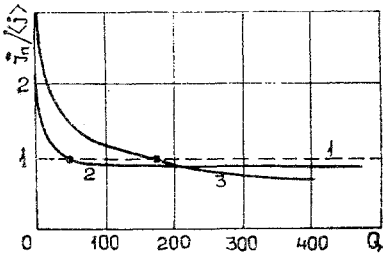

Fig. 12

the conductor $I = \int j dS$ and the voltage across the conductor. The signal from the voltage sensor is the sum of ohmic and inductive voltage drops $u_R + u_L$, $u_L = LdI/dt$, where L is the external inductance of the conductor. If we subtract the u_L component from the sensor signal, so that at the initial moment the difference signal is close to zero, then at subsequent times the value of this difference signal can be regarded as proportional to the voltage u_R, which when substituted in the expression $\tilde{Q} = \int I u_R dt$, will give the energy expended in heating the conductor, while substitution in $\tilde{R} = u_R/I$ gives the conductor resistance.

All this is true if the electric field and current density are uniformly distributed over conductor section. Then $u_R = El$, $I = jS$ (l is the conductor length, E is electric field, and S is conductor cross-sectional area), $\tilde{R} = El/jS = l/\sigma S$ and $\tilde{Q} = V \int j^2/\sigma dt$, where V is the volume of the conductor. Usually relative resistance $R = \tilde{R}/R_0$, $R_0 = l_0/\sigma_0 S_0$ is considered, where the quantities with zero subscripts refer to the initial moment of time. The quantity $\tilde{Q}$ is divided by either the initial conductor volume, or its total mass. In the latter case the specific internal energy Q will have dimensions of J/g.

The experimental graphs are simplest if the function R(Q) is constructed. Assuming that $R = \frac{\sigma_0}{\sigma}\frac{S_0}{S}\frac{l}{l_0}$, one can attempt to consider thermal expansion in the following manner: We assume either $S = S_0(1 + 2\alpha\Delta T)$ (where α is the linear thermal expansion coefficient, $l = l_0(1 + \alpha\Delta T)$), or $S = S_0(1 + 3\alpha\Delta T)$, while $l = l_0$. Further, not having exact solutions, one can assume some intermediate situation, since the first case corresponds to free expansion over all coordinates, while the second corresponds to free flow in the radial direction.

Then

$$R = (\sigma_0/\sigma)(1 - \varepsilon), \tag{3.1}$$

where $\varepsilon = (1 - 3)\alpha\Delta T$. Therefore, to the accuracy of ε, the value of R will reflect the behavior of conductivity. In this approximation the value of Q may be assumed proportional to the enthalpy, and the graph R(Q) can be regarded as a relationship between conductivity and enthalpy.

Such an interpretation is undoubtedly unjustifiable in the initial stage of the process at times of the order of the magnetic diffusion time. In experiment, the "resistance," constructed as $\tilde{R} = u_R/I$ falls with time in this period, and there is an upward spike in the R(Q) graph at the very beginning. These facts indicate that the sensor signal is proportional to the field on the conductor surface. However since in the coordinates (R, Q) the spike is localized near zero, this is not a problem because after several diffusion times pass one could at first glance assume that the current density distribution over radius has become uniform.

The fact that we measure not some effective ohmic resistance, for example, $R \sim \int j^2/\sigma dS / \int j^2 dS$, but rather a quantity proportional to electric field on the surface E_n also follows from experiments of the type of Fig. 1 with strong skin effect. Here

$$R = \frac{E_n l}{I}\frac{S_0\sigma_0}{l_0} = \frac{j_n}{\langle j\rangle}\frac{S_0}{S}\frac{l}{l_0}\frac{\sigma_0}{\sigma_n}. \tag{3.2}$$

This expression differs from Eq. (3.1) in the factor $j_n/\langle j\rangle$, where $\langle j\rangle$ is the mean current density over section, and j_n, σ_n are the current density and conductivity on the surface.

In the intense skin effect regime the current density on the surface may be less than the mean value because of higher surface temperature (see Figs. 1, 2) and the experimental R(Q) curve will intersect the "theoretical" straight line $\sigma(Q) = \sigma_n/\sigma_0$.

For regimes corresponding to case 1 of the table, where the characteristic heating time is significantly greater than the magnetic diffusion time, it is usually assumed that the experimental results can be interpreted with Eq. (3.1).

As follows from Sec. 1, consideration of the dynamics of expansion leaves no room for the case of uniform current density distribution. Therefore it is necessary to compare the calculation results with experiment, assuming that in experiment the total current and a voltage proportional to the electric field on the conductor surface were measured. Figure 10 shows calculated oscillograms of these signals. The current values are normalized relative to the current at the surface $(j_n - \langle j \rangle)/\langle j \rangle$. This quantity, initially positive ("normal" skin effect), changes sign after $2.7 \cdot 10^{-6}$ sec, goes to a level of —10%, then remains practically unchanged up to the current maximum ("reverse" skin effect, produced by the density profile of Fig. 3).

For comparison with experiment, Fig. 11 shows graphs in the coordinates (R, Q). The only adjustable parameter here is the scale coefficient of 1.08, which considers inaccuracies in the conductivity and state equations, as well as systemic errors in determining mass density at the conductor surface. This coefficient is selected such that at the fusion point the value of the relative conductivity change $\sigma_0/\sigma_n = 6.1$ (copper).

Line 1 corresponds to the function σ_0/σ_n; curve 1' is a graph of $\sigma_0 S_0/\sigma S$, where S is obtained by calculation, line 2 corresponds to variant 2 of the table, while line 3 is variant 3 with strong skin effect.

The behavior of these curves (rise at low energy levels, intersection of the various curves with each other and the "theoretical" straight line) agrees completely with actual experiments.

Quantitative agreement is shown by the experimental points obtained for explosion of an 0.5 mm diameter copper conductor in an electrical circuit with period of $\sim 38 \cdot 10^{-6}$ sec. Here fusion commences in $7.3 \cdot 10^{-6}$ sec, and the heating regime is close to variant 2 of the table. In Fig. 11 the graphs intersect with the straight line σ_0/σ. Figure 12 shows the character of current density redistribution over section for cases 2 and 3 of the table. The curves are constructed in coordinates $(j_n/\langle j \rangle, Q)$. Line 1 corresponds to uniform current density distribution $(j_n/\langle j \rangle = 1)$. The arrows indicate points at which the curves intersect the straight line in coordinates (R, Q). With relatively slow heating this intersection point is close to the point where the current density at the surface becomes lower than the mean value.

The results of our examination of the dynamics of impulsive metal heating by a current (Section 1) and the refinements made with regard to measurements allow solution of a number of problems involving anomalies in electrical explosion. The term anomaly is usually applied to facts discovered in experiment which are in some sense unexpected.

A significant number of experimental studies [18, 3, 19] have found that R(Q) curves, at least in the energy range corresponding to heating of the liquid phase to the boiling point and beyond, do not coincide in experiments with different heating rates. By varying the heating rate a family of nonintersecting curves can be obtained [19]. With increase in heating rate the curves move downward, and the characteristic points on the curve shift to the right. If, to interpret this fact on the basis of formula (3.1), it is assumed that the current density and the conductivity are distributed uniformly along the radius of the conductor, then it is natural to infer that the conductivity is not only a function of thermodynamic parameters, but also depends on the heating rate. It is natural to utilize the current density as a value characterizing the heating rate. It then develops that $\sigma = \sigma(j)$. However at current densities of $j \sim 10^7$ A/cm^2 deviations from Ohm's law caused by a difference between the electron kinetic and lattice temperatures should be negligibly small [20], and an attempt to interpret the experimental data with Eq. (3.1) leads to a paradox.

The use of accepted theoretical estimates here is not completely correct, since the latter are based on the conduction model of a solid body while we are actually concerned with a liquid. But experiment also indicates that similar ambiguity exists in the prefusion energy range [21]. In the majority of experiments the slope of the R(Q) curve for this region proves to be of the same order of magnitude as the random component of the measurement uncertainty.

In [5] the random uncertainty was reduced to 1-2%. The data processing problem was formalized, and the accuracies of the following determinations were found: slope of curve φ, coordinates of beginning ($\hat{R}_H$, $\hat{Q}_H$) and completion ($\hat{R}_K$, $\hat{Q}_K$) of fusion. One of the results of [5] is that the linear model provides a good approximation of the data, while the slope φ of this line is statistically significantly lower than the "theoretical" φ. In relative units, $\varphi - \hat{\varphi} = 0.77 \pm 0.17$. Thus, the anomaly is reproduced in the solid heating stage as well.

The explanation of this paradox in experiments with wires is that the current density, despite estimates obtained with the incompressible liquid model, is in fact distributed nonuniformly over section (see Fig. 6), mainly because of the dependence of conductivity on density. Under these conditions the quantity described by Eq. (3.2) is actually measured.

It is known that near the fusion point a liquid film forms on the surface of crystals. The total surface energy then decreases. As a consequence of the energetic favorability of liquid formation on the surface marked superheating of that surface under quasistationary conditions is practically impossible.

Studies of electrical explosion usually cite [22], where use of a strong air draft on the surface of a tin crystal ($T_f \cong 232°C$) hindered development of a liquid film, so that a superheating of 1-1.5°C was achieved. The citation of [22] is offered as proof that the amount of superheating can become measurable. Experimentally, superheating under equilibrium conditions should be recorded as a shift of the first inflection point of the R(Q) curve into the region to the right of the commencement of fusion Q^T, which is known to high accuracy from conventional measurements. In [2] there was a report of a shift to the right of the fusion point of lead ($T_f \cong 325°C$) by an anomalously large amount ($\sim 43°C$). The relative value of the shift in that case is only insignificantly more than the uncertainty level of the measurements and processing. A similar shift was recorded in copper wire experiments in [5]. The statistical significance of this result can be characterized by the following values. The position of the R(Q) inflection point on the energy axis $\hat{Q} = 525 \pm 7$ J/g. Under thermodynamic equilibrium conditions $Q^T = 475$ J/g, so that $\hat{Q} - Q^T = (50 \pm 7)$ J/g. If this shift is interpreted as superheating, its value is anomalously large ($\Delta T \sim 100°K$).

Such an interpretation rests on the invalid assumption that heating occurs under conditions of thermodynamic equilibrium. According to the results of the calculations performed, such an assumption is unrealistic even within the ideal compressible liquid model. In that same model the shift of the beginning of fusion to the right has at least a partial simple explanation, as follows.

The quantity $Q \sim \int u_R I dt$ calculated from experimental data, is proportional to the total energy passing through the external surface ($u_R \sim E_n$, $I \sim H_n$, $u_R I \sim E_n \times H_n$ is the Poynting vector). Kinetic and field energy may be neglected in comparison to thermal energy. Therefore the abscissa of the R(Q) curves actually represents a quantity proportional to the mean temperature over radius. The surface temperature may be more or less than this mean. The former case is realized at $t_h \ll t_m$ (see Fig. 2), the latter, at $t_h \gg t_m$ (Fig. 6). In Fig. 6, which reflects the time when the surface temperature is equal to the fusion point at atmospheric pressure, the mean temperature over radius is 10% higher (fusion point shifted to right on energy axis) and the mean current density over radius is 8% higher than on the surface (shift downward along R axis).

The data of Fig. 6 characterize a heating regime in which $t_h/t_m = 4$, and $t_m/t_s = 40$. In this regime calculation of temperature and current density profiles with the incompressible liquid model where $\sigma = \sigma(T)$ produces distributions practically uniform over radius. In the experiments of [5, 21] the second case was realized. The fusion point moves in the required direction if compressive forces produced by relaxation processes act upon the surface. Thus, the statement that superheating of a metal surface under equilibrium conditions in electrical explosion is impossible is unjustified.

Another anomaly reported many times, including [5], can also be explained naturally, namely, the shift to the right of the point at which fusion is completed. Depending on the algorithm used to determine the point, the amount of the shift is 70-120 J/g. A value of 70 ± 5 J/g [5] is obtained if the point is defined as the intersection of two straight lines obtained by smoothing the experimental data with the method of least squares, the first line being for the fusion region and the second, for the liquid region. The value of 120 J/g

corresponds to the minimum of the curve dR/dQ. We recall that we deal here with regimes in which $t_h \gg t_m$. This shift is inexplicable if isothermal fusion occurs within the volume.

In the model of a liquid—solid boundary moving from the surface into the specimen no other result is possible, since the entire fusion process occurs over a time significantly less than the thermal conductivity time, so that the heat liberated over the entire volume of the liquid phase with the exception of a thin boundary layer is not transferred to the phase conversion surface, but is expended in heating the liquid. A coarse estimate of the amount of the shift can be obtained by assuming that the heat source power density in the liquid is twice (for copper) as small as in the solid ($\sigma_s/\sigma_l = 2$, where σ_s and σ_l are the conductivities of solid and liquid phases at the fusion point). Then at the end of the fusion phase we may expect $\Delta Q = \lambda/2$, where $\lambda \cong 200$ J/g is the heat of transition.

The question of the character of the current density profile at the end of the fusion phase can be answered with practically no ambiguity by Eq. (3.2), since during the fusion phase the total current does not change. Since the surface conductivity is initially $\sigma_n = \sigma_s$, while at the end we have $\sigma_n \cong \sigma_l$, the current density at the surface increases with respect to the original value of $\hat{R}_K/\hat{R}_H \geqslant 2$, and falls, if $\hat{R}_K/\hat{R}_H < 2$. In experiment $\hat{R}_K/\hat{R}_H \cong 1.75 < 2$, i.e., the ratio of the current density on the surface to the mean at the end of fusion decreases as compared to its initial value. And since initially $j_n < \langle j \rangle$, the temperature profile at the completion of fusion cannot have a maximum at the surface.

We will estimate the value of the "magnetohydrodynamic" correction to Ohm's law, which in our case can be written as

$$\mathbf{j} = \sigma(\mathbf{E} + [\mathbf{u} \times \mathbf{H}]/c).$$

The velocity vector u is directed toward the surface, and the absolute value of u, just like that of the magnetic field H, increases linearly with radius in the first approximation. The electric field is thus equal to

$$E = \frac{j}{\sigma}\left(1 - \frac{u(1)\,H(1)\,r^2\sigma}{cj}\right).$$

The unknown quantity $\delta E/E = u(1)H(1)r^2\sigma/cj$, where $0 \leqslant r \leqslant 1$. For case 2 of the table on the surface ($r = 1$) $u = 500$ cm/sec, $H = 3.3 \cdot 10^5$ Oe, $j = 2 \cdot 10^7$ A/cm^2, $\sigma = 10^5$ $(\Omega \cdot \text{cm})^{-1}$. The quantity $j/\sigma = 200$ V/cm, while $uH/c = 1.5$ V/cm. Thus, $\delta E/E$ is of the order of magnitude of 1%.

To complete our discussion of anomalies, we note that we do not speak here of electrical explosion as a process which commences at a temperature greatly exceeding the equilibrium boiling point. In principle the relaxation pattern considered permits an increase in the calculated shear stress amplitudes through suitable selection of tangent relaxation times so that the pressure on the surface $p = -(\sigma_\varphi + \sigma_z)/3$ will ensure a shift in the temperature at which fusion commences to the explosion point as determined experimentally. However such a procedure appears too artificial when applied to a liquid.

The situation is different with respect to mass density, as a consequence of which there should be a nonequilibrium increase in mass density (pressure) on the liquid surface.

Additional data not presented here, yet of some interest, particularly with regard to the initial stage of the process, may be found in [23].

The authors are indebted to S. K. Godunov for his kind evaluation of the study.

LITERATURE CITED

1. G. A. Gemmerling, "Dependence of internal energy of a body on the rate of temperature change," Dokl. Akad. Nauk SSSR, 180, No. 5 (1980).
2. M. M. Martynyuk and G. É. Gerrero, "Measurement of electrical resistance and heat content of metals by the impulsive method," Zh. Tekh. Fiz., 42, No. 1 (1972).
3. I. F. Kvartskhava, V. V. Bondarenko, et al., "Oscilloscopic determination of electrical explosion energy," Zh. Eksp. Teor. Fiz., 31, No. 5 (1956).
4. S. G. Bodrov, M. L. Lev, and B. P. Peregud, "Flexion magnetohydrodynamic instability of a current-carrying conduction," Zh. Tekh. Fiz., 48, No. 12 (1978).
5. A. M. Iskol'dskii and V. S. Kirichuk, "Processing of experimental results described by a mathematical model with singular points," Avtometriya, No. 4 (1975).

6. L. D. Landau and E. M. Lifshits, Electrodynamics of Continuous Media [in Russian], Fizmatgiz, Moscow (1959).
7. S. K. Godunov, Elements of the Mechanics of Continuous Media [in Russian], Nauka, Moscow (1978).
8. S. K. Godunov, N. S. Kozin, and E. I. Romenskii, "Equation of state of elastic energy in metals with nonspherical deformation tensor," Zh. Prikl. Mekh. Tekh. Fiz., No. 2 (1974).
9. S. K. Godunov, V. V. Denisenko, et al., "Use of the relaxation viscoelasticity model for calculation of single-axis homogeneous deformations and refinement of Maxwell viscosity interpolation formulae," Zh. Prikl. Mekh. Tekh. Fiz., No. 5 (1975).
10. S. K. Godunov, A. V. Zabrodin, M. Ya. Ivanov, A. N. Kraiko, and G. P. Prokopov, Numerical Solution of Multidimensional Problems in Gas Dynamics [in Russian], Nauka, Moscow (1976).
11. A. P. Baikov and A. F. Shestak, "The character of metallic conductor fusion upon impulsive heating," Pis'ma Zh. Tekh. Fiz., 5, No. 22 (1979).
12. S. R. De Groot and P. Mazur, Non-equilibrium Thermodynamics, Elsevier (1962).
13. D. N. Zubarev and M. V. Sergeev, Supplement to W. A. Day's "Thermodynamics of Porous Media with a Memory" [Russian translation], Mir, Moscow (1974).
14. A. F. Shubin, V. P. Rotshtein, and D. I. Proskurovskii, "Plastic deformation of a metal under the action of an intense electron beam 10^{-8}-10^{-7} sec in duration," Izv. Vyssh. Uchebn. Zaved., Fiz., No. 7 (1974).
15. V. P. Rotshtein, L. S. Bushnev, and D. I. Proskurovskii, "Dislocation structure of copper irradiated by an intense electron beam 10^{-8}-10^{-7} sec in duration," Izv. Vyssh. Uchebn. Zaved., Fiz., No. 3 (1975).
16. V. P. Knyazev and G. A. Shneerson, "Study of rapid expansion of thin wall metal cylinders in an intense magnetic field," Zh. Tekh. Fiz., 40, No. 2 (1970).
17. L. M. Shestopalov, Deformation and Plasticity Waves in Metals [in Russian], Akad. Nauk SSSR, Moscow (1958).
18. V. A. Burtsev, N. V. Kalinin, and V. N. Litunovskii, Electrical Explosion of Conductors [in Russian], NIIEFA D. V. Efremov, Leningrad (1977).
19. A. P. Baikov, L. S. Gerasimov, and A. M. Iskol'dskii, "Experimental study of metal foil conductivity during electrical explosion," Zh. Tekh. Fiz., 45, No. 1 (1975).
20. V. L. Ginzburg and V. P. Shabanskii, "Kinetic temperature of electrons in metals and the electron emission anomaly," Dokl. Akad. Nauk SSSR, 100, No. 3 (1955).
21. A. P. Baikov, A. M. Iskol'dskii, and Yu. E. Nesterikhin, "Electrical explosion of wires at high energy input rates," Zh. Tekh. Fiz., 43, No. 1 (1973).
22. S. É. Khaikin and N. P. Béne, "On the phenomenon of superheating in a solid," Dokl. Akad. Nauk SSSR, 23, No. 1 (1939).
23. V. N. Dorovskii, A. M. Iskol'dskii, and E. I. Romenskii, "Dynamics of impulsive metal heating by a current and electrical explosion of conductors," Preprint No. 174, Inst. Avtomatiki Elektromet., Sib. Otd. Akad. Nauk SSSR, Novosibirsk (1982).